# Simulated formation of UV-cured polymer lenses on aqueous substrates

Robert Thompson[a,*], Simon Hempel-Costello[b], Zack Johnson[b], Emily K. Schwartz[b], Samuel Stevenson[b], Eleanor Weston[b], and Martha-Elizabeth Baylor[b]

[a]Department of Mathematics and Statistics, Carleton College, Northfield, MN, USA
[b]Department of Physics and Astronomy, Carleton College, Northfield, MN, USA

## ABSTRACT

We simulate the formation of macroscopic polymer lenses made by depositing a hydrophobic liquid polymer on an aqueous substrate, and explore how changing the hydrophobicity of the polymer affects lens shape. Methods for the fabrication of polymer lenses and the measurement of interfacial tensions between polymer, substrate and air are described. Characteristics of simulated and fabricated lens shapes are compared. Finally we indicate possible obstacles to the use of simulations for predicting properties of polymer lenses made with this technique.

**Keywords:** photopolymers, lenses, surface tension, Young-Laplace equation

## 1. INTRODUCTION

Polymers present an appealing alternative to glass in the manufacturing of optical components due to lower density and fabrication costs. Traditional technologies rely on molds for polymer lens creation: polymer is dispensed into the mold and cured, taking on the shape of the mold.[1] This allows manufacturers to replicate specific lens shapes, but microscopic flaws in the mold cast defects onto the lenses. It may be difficult to remove these defects, since heat from polishing can warp the lenses. So these mold-based methods of lens fabrication can result in flawed optical pieces. 3D printing of lenses is emerging as a more quickly customizable alternative to mold based methods. Printers are limited in surface quality, though improvements are being made with two-photon printing[2] and stereolithography.[3] Yet another alternative to molds is the use of surface tension to manipulate drops of resin into lens shapes.[4–6] Because the lens surfaces form at interfacial boundaries between air, polymer, and substrate, manufacturing defects in the lens surfaces can be reduced or eliminated. Until recently, surface tension techniques were limited to the micro-scale. However, Falahati, et al.[7] uses magnetic liquid to control the shape of macro lenses and Elgarisi, et al.[8] uses fluidic shaping to create optical components that are not size limited. Both molds and 3D printers allow direct control over the size and shape of the lenses while the surface tension methods require a model to predict lens dimensions. Thus, research groups are creating simulations to predict lens shapes fabricated using these surface tension methods.[9,10]

In this work, we simulate the formation of smooth polymer lenses created via deposition of a hydrophobic liquid polymer onto an aqueous substrate. Factors such as interfacial tensions and densities of the polymer and substrate, as well as wetting, liquid volumes, and containers used for manufacturing determine the shape of a lens. The fabrication method we use was originally developed by Zimmerman, et al.[11] and is similar to the micro-lens creation process of Sun, et al.,[12] which they also simulated.[10] Our simulation process is based on Burton, et al.,[9] and allows for simulation of macroscopic lenses.

The paper is structured as follows. We derive the model for simulating lens formation first in Section 2, then discuss our lens fabrication process in Section 3. Measurement of physical parameters necessary for the simulation is described in Section 4. Finally, we compare characteristics of modeled and fabricated lenses in Section 5.

Corresponding author: Robert Thompson rthompson@carleton.edu

## 2. MODELING LENS FORMATION

To model the formation of a liquid lens, we employ the axisymmetric Young-Laplace equation,

$$\Delta P = 2H\sigma - \Delta\rho g z, \tag{1}$$

which describes the shape of an interface between two fluids at equilibrium.[9,13] In this equation, $\Delta P$ is the pressure difference across the interface, $\Delta\rho$ is the density difference across the interface, $H$ is the mean curvature of the interface, $\sigma$ is the interfacial tension of the interface, and $g$ is gravitational acceleration. With these parameters known, Eq. (1) is a partial differential equation which can be solved to determine the interface shape in axisymmetric coordinates $r, z$.

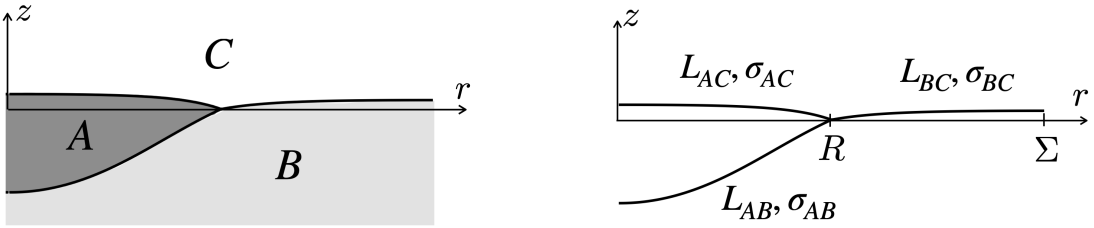


Figure 1: A radial cross section of a liquid lens showing the three interfaces and some parameters associated with these interfaces. $A$ refers to the photopolymer resin, $B$ refers to the substrate, $C$ refers to air. $L_{AB}$,$L_{BC}$, and $L_{AC}$ refer to the length of each interface and $\sigma_{AB}$, $\sigma_{BC}$, and $\sigma_{AC}$ refer to the interfacial tensions along each interface. $R$ is the radius of the lens and $\Sigma$ is the radius of the substrate container.

We use letters $A, B, C$ to indicate quantities associated with resin, substrate, and air, respectively. Our lens has three interfaces governed by the Young-Laplace equation: resin-substrate ($AB$), substrate-air ($BC$), and resin-air ($AC$). Because of symmetry, a single radial cross section, as shown in Fig. 1, suffices to describe the entire lens. Following Burton, et al.,[9] our strategy for determining a lens shape is to numerically solve Eq. (1) for each of these interface curves subject to pressure and force balance conditions where the three interfaces meet.

We let $(r(s), z(s))$ be the parameterization of any one of these three interface curves, with $L$ as the total length of this curve. Here $s$ is a unitless constant speed parameter with speed $\sqrt{r'(s)^2 + z'(s)^2} = L$, where $s = 1$ corresponds to the intersection point of the interfaces and $s = 0$ is either the center of the lens or the wall of the container (depending on which interface is considered). Combining this parameterization assumption with an explicit expression for the mean curvature $H$ yields a system of second order ordinary differential equations for $r(s)$ and $z(s)$:

$$r''(s) = z'(s)\left(\frac{L\Delta P}{\sigma} - \frac{L\Delta\rho g z(s)}{\sigma} + \frac{z'(s)}{r(s)}\right), \qquad z''(s) = -r'(s)\left(\frac{L\Delta P}{\sigma} - \frac{L\Delta\rho g z(s)}{\sigma} + \frac{z'(s)}{r(s)}\right). \tag{2}$$

Note that there are three such systems; one for each of the interfaces $AB$, $AC$ and $BC$.

We let $\Sigma$ be the radius of the substrate container, $R$ the radius of the lens, and $V$ the volume of the lens. For initial conditions, we take

$$r_{AB}(0) = r_{AC}(0) = 0, \quad r_{BC}(0) = \Sigma, \quad r'(0) = L, \quad z(0) = 0, \quad \text{and} \quad z'(0) = 0. \tag{3}$$

We impose the conditions $z(0) = 0$ without loss of generality by requiring that the interfaces be shifted after the numerical solution process to align the three curves at their common intersection point. The parameters $V$, $\Delta\rho_{AB}$, $\Delta\rho_{BC}$, $\Delta\rho_{AC}$, $g$, $\Sigma$, $\sigma_{AB}$, $\sigma_{BC}$ and $\sigma_{AC}$ are either preset in the fabrication process or determined via measurement. We discuss this measurement in depth in Section 4. The parameters $R, \Delta P_{AB}, \Delta P_{BC}, \Delta P_{AC}$, $L_{AB}$, $L_{BC}$, and $L_{AC}$ are determined during the simulation process. We solve Eqns. (2) numerically via a shooting method as follows:

1. Guess values for the unknown parameters $R, \Delta P_{AB}, \Delta P_{BC}, \Delta P_{AC}$, and $L$.

2. Numerically solve Eqns. (2) using the guessed values above, the known values for $\Delta\rho_{AB}$, $\Delta\rho_{BC}$, $\Delta\rho_{AC}$, $g$, $\Sigma$, $\sigma_{AB}$, $\sigma_{BC}$, $\sigma_{AC}$ and the initial conditions (3).
3. Using the numerical solutions from 2., test for force and pressure balance at $s = 1$, and test that the lens volume has the desired value $V$.
4. If the conditions in 3. are satisfied, accept the solutions as a valid lens. If they are not, return to 1.

We next describe the procedures used to fabricate polymer lenses similar to those described by this model.

## 3. LENS FABRICATION

Our lens fabrication process follows the methods of Zimmerman, et al.[11] as shown in Fig. 2. We create ten identical bored wells of radius $\Sigma = 0.375$ in (9.525 mm) and height $h = 25$ mm in an acrylic block. We fill these wells with our substrate, distilled water, to a depth of $s = 24$ mm. We use a micropipette to deposit 0.2 mL of hydrophobic photopolymerizable resin into each well, forming a lens-shaped droplet on the substrate surface. We then cure the resin via UV light (Bacchus and Associates LS-100-2) with intensity 38.5 mW/ cm$^2$ at 365 nm for 310 s.

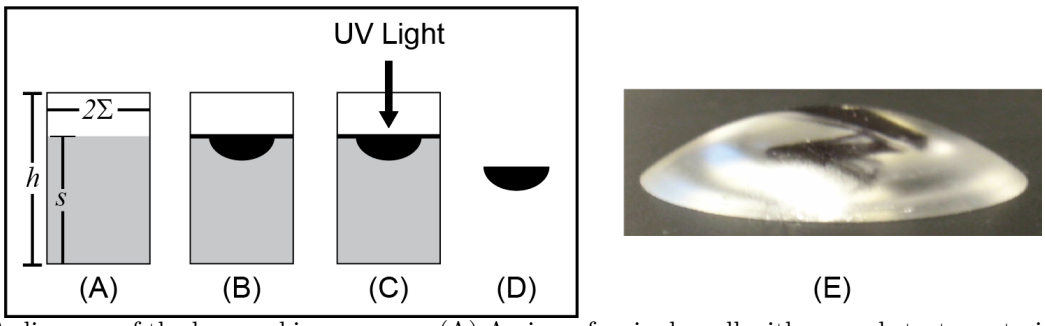


Figure 2: A diagram of the lens making process. (A) A view of a single well with our substrate material, distilled water. Labeled are the height of the well $h$, the depth of the water $s$, and the diameter of the well in terms of the simulation parameter $\Sigma$. (B) When we add resin to the water, the resin forms a lens-shaped object in the center with a thin film of resin that reaches to the edge of the container. (C) UV light is shown on the resin so that it is cured to a glassy state. Due to oxygen-inhibition, the thin film does not cure. (D) The resulting solid lens after removal from the water. (E) A photo of the resulting lens.

During deposition there is pseudopartial wetting, resulting in a thin film of resin on the water surface.[14] Because of oxygen inhibition (i.e., the process by which the presence of oxygen prevents free-radical polymerization),[15] oxygen diffusion at the surface of the resin prevents a thin film of resin from curing. At the center of the container, the resin is thick enough that UV light is able to promote polymerization faster than oxygen can diffuse into the bulk of the resin, allowing the creation of a lens-shaped object. A thin liquid film remains on the air-resin surface of the lens after curing. We remove the film using a small amount of acetone, which does not damage the cured lens. We clean the acrylic wells using a cycle of soap, water, and methanol. We fabricate all lenses at room temperature with less than 2°C variation. A single person fabricates lenses to avoid systematic shifts in data observed when different researchers pipette resin.[11]

We measure the shape of a cured lens by projecting a profile of the lens using a collimated Helium-Neon laser. We capture an image of the profile, and we find the upper boundary of the lens via image segmentation in MATLAB (see Fig. 3(A)). We fit a parabola to this lens profile via least-squares (see Fig. 3(B)) and we find the height $H_E$ and width $W$ from the parabolic fit parameters (see Fig. 3(C)). Note that due to the measurement method where we are unable to see the shallow curvature side of the lens, we only measure the height $H_E$ of the upper portion of the lens, not the full height $H_M$.

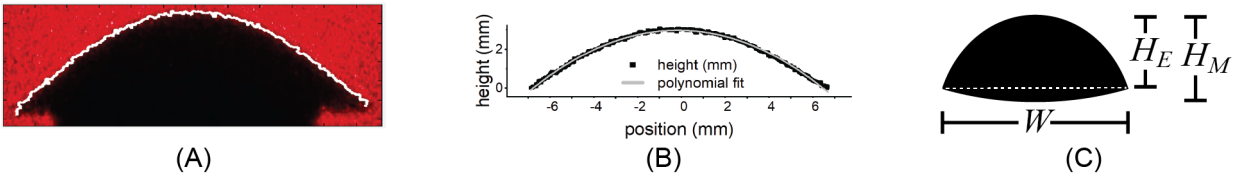


Figure 3: Characterization of a lens profile. (A) Image of a lens profile as recorded by a camera looking at a frosted glass plate where collimated laser light is incident on a lens sitting on a pedestal. Software traces the surface of the lens (white). (B) We fit the surface trace using a parabolic function. (C) We use the polynomial fit to determine the height to width ratio HWR= $H_E/W$.

## 4. MEASURING INTERFACIAL TENSIONS

We use a translucent, hydrophobic resin custom made for our lab by Colorado Photopolymer Solutions, composed of 80% tricyclodecanedimethanol diacrylate (TCDDA), 20 % phenethylamine (PEA), and 0.5% Diphenyl (2,4,6-trimethylbenzoyl) phosphine oxide - liquid (TPO-L) as the photoinitiator at 365nm. We use a fluorinated acrylate (CN4004) to alter the hydrophobicity of the resin. Thus CN4004 changes the surface tension for the resin/water ($\sigma_{AB}$) and resin/air interface ($\sigma_{AC}$). We measured these changes in surface tension via a pendant-drop method which we now describe.

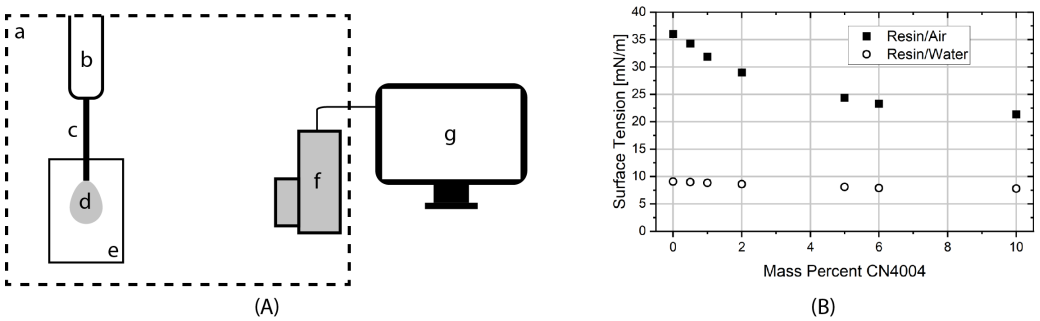


Figure 4: (A) Measurement of surface tension via the pendant drop method: (a) Attension Theta tensiometer, (b) Hamilton 1700 series syringe; (c) syringe tip; (d) resin drop; (e) container of air or water; (f) camera; (g) One Attension v. 3.2 software and (B) the resulting values of resin-air and resin-water surface tension. Error bars, removed for clarity, are $\leq \pm 0.5$mN/m for each value.

To measure $\sigma_{AC}$, we dispense a droplet of resin from a Hamilton 1700 series syringe needle of known diameter into the air as shown in Fig. 4(A). We use an Attension Theta tensiometer by Biolin Scientific, taking approximately 10 images per second. These images are processed via One Attension v.3.2 to determine surface tension values. We measure $\sigma_{AB}$ similarly by suspending the resin droplet in a cuvette of distilled water. Resin-water diffusion affects measured surface tension, and this effect diminishes after approximately 60 seconds, so we begin taking surface tension measurements 60 seconds after the drop is initially exposed to the water. We take averages of multiple drops for each resin variation to determine uncertainty in the measurements. Fig. 4(B) shows measurements of surface tension versus concentration of CN4004 for resin-air and resin-water interfaces.

As previously mentioned, pseudo-partial wetting occurs during lens fabrication, resulting in a thin film of resin on the water surface. This alters the air-substrate surface tension ($\sigma_{BC}$) from what we would expect with water as our substrate. To attempt measurement of this modified $\sigma_{BC}$, we used a Wilhelmy Plate System from Riegler & Kirstein.[16] The wells of the lens fabrication container are too small to properly measure the surface tension along the $BC$ interface, so we filled a larger beaker (three times the well diameter) with distilled water and measured $\sigma_{BC}$ after depositing droplets of resins with varying $\sigma_{AC}$ (from 23.30mN/m to 36.00mN/m). The resulting $\sigma_{BC}$ values varied between 47 and 65mN/m, significantly lower than the typical air-water value of approximately 72mN/m. These reduced values did not produce reliable numerical results, but strongly suggest a value of $\sigma_{BC}$ well below 72mN/m. Furthermore, because of the larger diameter container used in this measurement, we believe

the film is potentially thicker under fabrication conditions, so that the actual air-substrate surface tension during fabrication would be smaller. Based on these observations, we explored even lower $\sigma_{BC}$ values in our simulation.

## 5. RESULTS

In this section we compare fabricated lenses with those obtained through simulation using similar physical parameters. Of primary interest is a comparison of the ratios of $H_E$ to $W$ (HWR) and the range of focal lengths for simulated lenses. We fabricate lenses for different levels of CN4004 and determine HWR for these lenses as described in Section 3. The measurements described in Section 4 provide values for the resin-air surface tension $\sigma_{AB}$ and resin-substrate surface tension $\sigma_{AC}$ for the given levels of CN4004. Parameters needed for simulation are shown in Table 1. We use values of $\rho_B = 1$ kg/L for water density, $\rho_C = 0$ kg/L for air density, and $g = 980.665$ cm/s$^2$ throughout.

Table 1: Parameter values appearing in lens simulations.

| Parameter | Value | Source | | Parameter | Value | Source |
|---|---|---|---|---|---|---|
| $V$ | 0.2 mL | experimentally set | | $L_{AB}$, $L_{BC}$, $L_{AC}$ | varies | simulation output |
| $\Sigma$ | 0.375 in | experimentally set | | $\sigma_{AB}$, $\sigma_{AC}$ | varies | measured |
| $\rho_A$ | 1.056 kg/L | experimentally set | | $\sigma_{BC}$ | varies | computationally varied |
| $R$ | varies | simulation output | | $\Delta P_{AB}, \Delta P_{AC}, \Delta P_{BC}$ | varies | simulation output |

As discussed in Section 4, the air-substrate tension $\sigma_{BC}$ is likely to be substantially smaller than the typical air-water tension of 72mN/m at standard temperature and pressure due to pseudo-partial wetting. We speculate that the actual air-substrate tension may be related to air-resin tension, since a thin resin film covers the air-water interface. We explore simulations for values of $\sigma_{BC}$ in the range of $\sigma_{AC}$, varying from $\sigma_{BC} = 26$mN/m to $\sigma_{BC} = 36$mN/m, observing trends as $\sigma_{AC}$ (i.e. CN4004 content) varies.

Fig. 5 shows the values of HWR for simulated and fabricated lenses for these various values of $\sigma_{BC}$, as well as focal lengths for simulated lenses. Higher values of $\sigma_{BC}$ than those displayed here tend not to produce valid lenses during simulation. HWR values clearly trend upward as $\sigma_{AB}$ increases and match well with experimental results for simultaneously low or high values of $\sigma_{AC}$ and $\sigma_{BC}$. Attainable simulated focal lengths vary from roughly 0.1 to 1.3cm, trending downward as $\sigma_{AC}$ increases. HWR comparison with fabricated lenses suggests that a similar range of focal lengths may be attainable by varying CN4004 content.

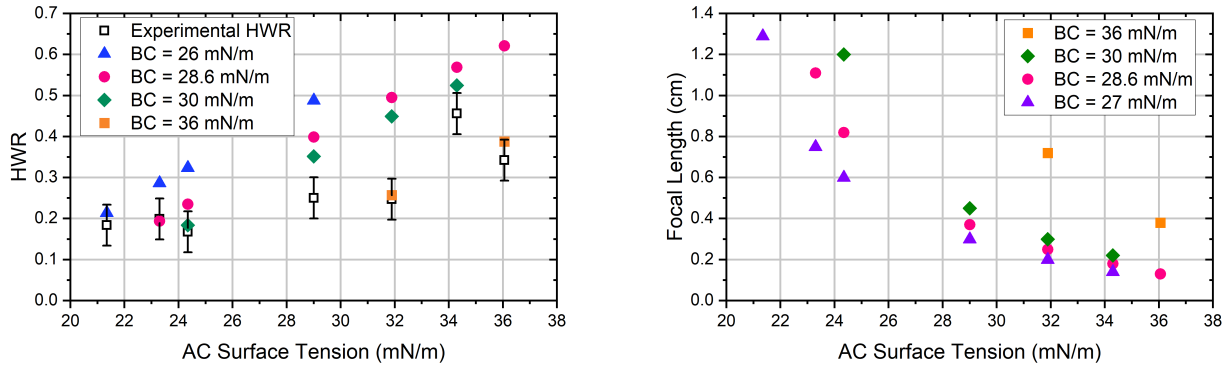


Figure 5: Graphs based on simulated data. (A)HWR vs AC surface tension for simulated lenses with comparison to fabricated lenses. (B) focal lengths of simulated lenses vs AC surface tension.

Fig. 6 shows a fabricated lens profile overlaid with the profile of a simulated lens with $\sigma_{AB} = 7.9$mN/m, $\sigma_{AC} = 23.3$mN/m, and $\sigma_{BC} = 28.6$mN/m. The profiles match well at the center, but deviate toward the outer edge. This deviation suggests that there may be inaccurate assumptions in the modeling process that become

more apparent near the interface of resin, air and substrate. One possibility is that the tension $\sigma_{BC}$ is not constant along the BC interface due to changes in the thickness of the thin resin film.

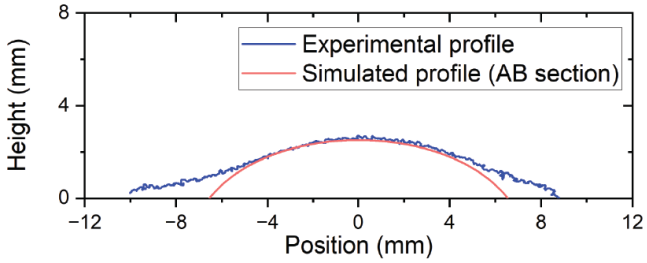


Figure 6: Simulated profile over the measured profile of the fabricated lens. Note that since the measured profile does not capture the AC interface of the lens, we only compare the AB portions of the profiles.

## 6. CONCLUSION

This paper seeks to bring together experimental practice and theoretical modeling to better understand limitations and opportunities for this fabrication technique for photopolymer lenses. We found that measurement of surface tension values is critical to the predictive power of the simulations. In particular, the value of air-substrate surface tension $\sigma_{BC}$ required to form simulated lenses appears to be much lower than the nominal surface tension of water. Future work will seek to understand how mixing of the resin with water during the wetting process impacts $\sigma_{BC}$, and use this understanding to better align simulation and fabrication results. Better measurements of fabricated lens profiles will also allow for a better comparison of the geometry of simulated and fabricated lenses. With reliable predictive power in our simulation, we envision a computational determination of the necessary physical parameters for creating lenses with desired properties for different optical applications.

## 7. ACKNOWLEDGEMENTS

The authors thank Dr. Benjamin Stottrup of Augsburg University for guidance, consult, and access to his tensiometer and Wilhelmy Plate System; Mark Zack, Aaron Heidgerken-Greene, Tom Baraniak, Paul Bernhardt, and Issa Wilson for their technical expertise and equipment support; Neil Cramer of Colorado Photopolymer Solutions for polymer resin formulations and the CN4004 additive; and Charlotte Zimmerman, Mason White, and Amy Sullivan for helpful conversations. This research was funded in part by the Harry A. and Margaret D. Towsley Foundation, the Carleton College department of Physics and Astronomy, and the Carleton College Department of Mathematics and Statistics.

## REFERENCES

[1] Peixoto, C., Valentim, P. T., Sousa, P. C., Dias, D., Araújo, C., Pereira, D., Machado, C. F., Pontes, A. J., Santos, H., and Cruz, S., "Injection molding of high-precision optical lenses: A review," *Precision Engineering* **76**, 29–51 (2022).

[2] Gissibl, T., Thiele, S., Herkommer, A., and Giessen, H., "Two-photon direct lazer writing of ultracompact multi-lens objectives," *Nature Photon* **10**, 554–560 (2016).

[3] Berglund, G. D. and Tkaczyk, T. S., "Fabrication of optical components using a consumer-grade lithographic printer," *Optics Express* **27**(21), 30405–30420 (2019).

[4] Xie, D., Zhang, H., Shu, X., and Xiao, J., "Fabrication of polymer micro-lens array with pneumatically diaphragm-driven drop-on-demand inkjet technology," *Optics Express* **20**(14), 15186–15195 (2012).

[5] Zhu, X., Zhu, L., Chen, H., Yang, M., and Zhang, W., "Fabrication of multi-scale micro-lens arrays on hydrophobic surfaces using a drop-on-demand droplet generator," *Optics & Laser Technology* **66**, 156–165 (2015).

[6] Nakazawa, S., Hitai, H., and Tokura, K., "Photopolymerization of spherical objects using interface tension between liquids," *Journal of the Japan Society for Precision Engineering* **68**(4), 571–575 (2002).

[7] Falahati, M., Zhou, W., Yi, A., and Li, L., "Fabrication of polymeric lenses using magnetic liquid molds," *Applied Physics Letters* **114**(20), 203701 (2019).

[8] Elgarisi, M., Frumkin, V., Luria, O., and Bercovici, M., "Fabrication of freeform optical components by fluidic shaping," *Optica* **8**(11), 1501–1506 (2021).

[9] Burton, J., Huisman, F., Alison, P., Rogerson, D., and Taborek, P., "Experimental and numerical investigation of the equilibrium geometry of liquid lenses," *Langmuir* **26**(19), 15316–15324 (2010).

[10] Sun, R., Falahati, M., and Li, L., "Numerical and experimental study on multiphase printing of polymeric biconvex micro lenses," *Journal of Micromechanics and Microengineering* **28**(11), 115005–115013 (2018).

[11] Zimmerman, C., White, M., and Baylor, M.-E., "Effects of varying interfacial surface tension on macroscopic polymer lenses," *Optical Engineering* **54**(9), 097108 (2015).

[12] Sun, R., Li, Y., and Li, L., "Rapid method for fabricating polymeric biconvex parabolic lenslets," *Optics Letters* **39**(18), 5391–5394 (2014).

[13] Cabezas, M. G., Bateni, A., Montanero, J. M., and Neumann, A. W., "Determination of surface tension and contact angle from the shapes of axisymmetric fluid interfaces without use of apex coordinates," *Langmuir* **22**(24), 10053–10060 (2006).

[14] Sebilleau, J., "Equilibrium thickness of large liquid lenses spreading over another liquid surface," *Langmuir* **29**(39), 12118–12128 (2013).

[15] O'Brien, A. K., Cramer, N. B., and Bowman, C. N., "Oxygen inhibition in thiol–acrylate photopolymerizations," *Journal of Polymer Science Part A: Polymer Chemistry* **44**(6), 2007–2014 (2006).

[16] Ebnesajjad, S., [*Handbook of Adhesives and Surface Preparation*], ch. Surface Tension and Its Measurement, 25–28, Elsevier (2011).